Acoustical Holography Imaging of Full-Scale Jet Noise Fields[a]

Alan T. Wall
Kent L. Gee
Tracianne B. Neilsen
Brigham Young University
N283 ESC
Provo
UT 84602
alantwall@gmail.com

Michael M James
Blue Ridge Research and Consulting
15 W Walnut Street
Asheville
NC 28801

ABSTRACT

Characterization of the large-scale turbulent structures of jet noise sources can lead to improved noise diagnosis and reduction methods. Array-based inverse methods, in conjunction with equivalent-wave models of the field, are useful for imaging source and radiation properties. In this work, acoustical holography methods are used to reconstruct the three-dimensional sound field of a jet from the installed engine on a military fighter aircraft. The jet was measured in the presence of a rigid reflecting plane (a concrete run-up pad), and the equivalent wave model incorporates this effect with an image source representation of the field. Reconstructions are used to investigate jet source distributions and radiation properties.

1. INTRODUCTION

THE primary noise source from a military jet-propelled aircraft is the hot, turbulent, supersonic exhaust plume (i.e., the "jet").[1] Jet noise poses a significant hearing loss risk to military personnel. It also may lead to community annoyance, school disruption, sleep disturbance and other health risks, and may negatively impact wildlife.[2] Noise reduction technologies and the development of operational procedures that minimize noise exposure are enhanced by the accurate characterization of noise sources within a jet.

In array-based acoustical inverse methods, a sound field (at a single frequency) is represented by a linear combination of spatial basis functions, or an expansion of wave functions, that obey the Helmholtz equation. To obtain a weighted set of functions that accurately represents the field radiated by a given source, the coefficients of these functions are found to match the expansion to acoustic quantities at a set of measurement locations in the field, often over a two dimensional surface. Then the field at another location is estimated from the sum of the weighted functions evaluated at the new position; this is referred to as the reconstruction. The accuracy of a sound field reconstruction from an inverse method relies heavily on (1) the ability of the wave functions to represent the field (completeness), and (2) the ability of the measurement to capture enough of the spatial variation in the acoustic field to represent each expansion function.

Statistically optimized near-field acoustical holography (SONAH)[3-5] is the imaging method that is the starting point for the method employed in this work. SONAH was developed to

---

reconstruct a total sound field from a truncated (patch) hologram measurement (similar to the Helmholtz equation least-squares, or HELS,[6-9] method). The SONAH algorithm is used to calculate a transfer function matrix between all hologram locations and reconstruction locations, then applies these transfer functions to the measured sound pressures. For example, a SONAH algorithm was applied to a laboratory-scale jet, in which cylindrical basis functions were used to represent the field.[10] For a second example, a SONAH formulation based on a plane-wave expansion of the field was applied to full-scale jet measurements as a first attempt at holographic reconstruction.[11] Hald[12] developed a SONAH method that relied on measurements of two parallel planar arrays to separate incoming and outgoing waves by concatenating two matrices of wave functions, one for each direction.

The transfer-function formulation of the SONAH algorithm allows for a convenient representation of the sound field, because multiple sets of wave functions can be included in the generation of the transfer function matrix through a concatenation scheme similar to that of Hald.[12] The flexibility of the SONAH method in allowing for multiple sets of elementary wave functions is important in the context of the present work. The full-scale jet studied herein was, of necessity, measured over a concrete run-up pad.[13] This introduced an interference pattern from a rigid boundary into the measured data, rendering a straightforward cylindrical representation of the jet inaccurate. Hence, a modified approach to SONAH, using a set of cylindrical functions for both the jet and its image source, has been found to be best suited to the geometry of the experiment.

The sound field reconstructed from this model is more accurate than the fields produced by NAH methods that do not incorporate a model of the ground reflection,[14,15] or do not account for the geometrical spreading of the field.[11] In the general case, this method, called multisource-type representation SONAH (MSTR SONAH),[16] employs a wave field expansion where the field is represented as a combination of multiple sets of elementary wave functions, each set for a single source shape and location. Inasmuch as the elementary wave functions conform well to each source shape, the total expansion is an accurate model for that source configuration. In this paper, MSTR SONAH is used to reconstruct the sound field of a jet from full-scale military aircraft.

2. THEORY

A detailed formulation of the MSTR SONAH algorithm is provided by Wall.[17] In summary, a set of wave functions, $\Psi_q, q = 1,2,\dots,Q$ are chosen, which fulfill the homogeneous Helmholtz equation in the source-free field, defined for a single frequency. The wave functions can be elementary functions of plane, cylindrical, or spherical waves, or they can be derived from knowledge of the source properties (outside the source-free region). For the SONAH algorithm, it is desirable to be able to express complex pressures at both the hologram locations and at the reconstruction locations as linear combinations of the same basis functions, Ψ_q. This is formulated as a matrix $\mathbf{A}$ of Q wave functions evaluated at a set of measurement points, and a second matrix $\boldsymbol{\alpha}$ of the same Q wave functions at a set of reconstruction points. In the MSTR SONAH algorithm, multiple sets of wave functions, one for each mth source, are generated in the matrices $\mathbf{B}_m$ and $\boldsymbol{\beta}_m$ for the measurement and reconstruction locations, respectively. The matrices of all M sources are concatenated to give

$$\mathbf{A} = \begin{bmatrix} \mathbf{B}_1 \\ \mathbf{B}_2 \\ \vdots \\ \mathbf{B}_M \end{bmatrix}, \text{and} \quad \boldsymbol{\alpha} = \begin{bmatrix} \boldsymbol{\beta}_1 \\ \boldsymbol{\beta}_2 \\ \vdots \\ \boldsymbol{\beta}_M \end{bmatrix}. \tag{1}$$

These matrices are then inputs for the traditional SONAH algorithm.[3,4]

The MSTR SONAH formulation for the current experiment employs two sets of cylindrical wave functions. Elementary cylindrical wave functions at a given location **r** are defined by

$$\Phi_{k_z,n}(\mathbf{r}) = \Phi_{k_z,n}(r,\phi,z) \equiv \frac{H_n^{(1)}(k_r r)}{H_n^{(1)}(k_r r_s)} e^{in\phi} e^{ik_z z}, \quad r \geq r_0, \tag{2}$$

where $H_n^{(1)}$ is the nth-order Hankel function of the first kind, r_s is some small reference radius (traditionally the assumed source radius), and the radial wavenumber is dependent on the axial wavenumber, k_z, by

$$k_r = \begin{cases} \sqrt{k^2 - k_z^2}, & for\ |k| \geq |k_z|, \\ i\sqrt{k_z^2 - k^2}, & for\ |k| < |k_z|, \end{cases} \tag{3}$$

where $k = \omega/c$ is the angular frequency and $c = 343$ m/s is the ambient sound speed. In this experiment, Hankel functions of order $n = 0$ are used. Equation (2) is evaluated at all hologram locations with respect to two cylindrical "origins" to form $\mathbf{B}_1 = [\Phi_n^1(|\mathbf{r}_h - \mathbf{r}_0^1|)]$ and $\mathbf{B}_2 = [\Phi_n^2(|\mathbf{r}_h - \mathbf{r}_0^2|)]$, where $\mathbf{r}_0^1 = (x_0^1, y_0^1, z_0^1) = (0, d, 0)$ m defines the point that is located at $z = 0$ and is collinear with the centerline of one extended source, and where $\mathbf{r}_0^2 = (x_0^2, y_0^2, z_0^2) = (0, -d, 0)$ m defines the point that is located at $z = 0$ and is collinear with the second source centerline. Then, $\mathbf{B}_1$ and $\mathbf{B}_2$ are concatenated to form the complete hologram wave function matrix, $\mathbf{A}$, as in Equation (1). A similar process is implemented to form the complete reconstruction wave function matrix, $\boldsymbol{\alpha}$.

3. EXPERIMENT

A detailed description of the full-scale jet measurement used here is provided by Wall,[13] and are summarized here. Holographic measurements were taken in the vicinity of an F-22A Raptor, with one engine operating at military power, and the other engine held at idle. Figure 1 describes the field measurement locations relative to the aircraft. Planes 1 and 2 were measured by a roving field array, parallel to the estimated shear layer boundary, in a series of scans each covering an area about 2 m by 24 m. The data at plane 2 are used as the hologram in this study. Plane 1 is used as a benchmark measurement for reconstruction accuracy, and plane 3 is not used in this part of the study. In addition, measurements were made along the arc shown in Figure 1 with the field array at seven locations, which data are also used as a benchmark.
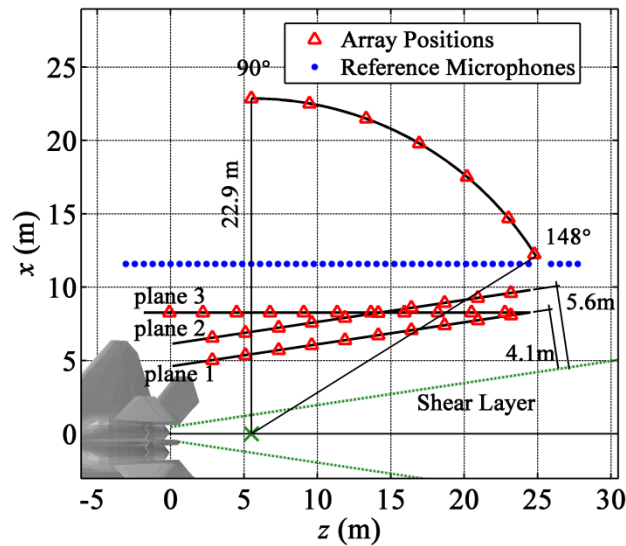
Figure 1: Schematic of the measurement locations, relative to the aircraft. The estimated shear layer boundary is marked by green dashed lines, and the green "x" delineates the estimated maximum noise source region and the center of the arc.

Prior to holographic reconstruction, a partial field decomposition was performed to generate coherent holograms from the scan-based measurements.[18] Then, since the measurement aperture was insufficient to capture the entire source at low frequencies (below about 200 Hz), the data were extrapolated numerically to estimate the data beyond the aperture.[19] Finally, reconstructions were made by projecting the extended, coherent, plane 2 data into the three-dimensional field using MSTR SONAH, with $d = 1.9$ m, the height of the jet centerline.

4. RESULTS

The results are shown first for the reconstruction of the 125 Hz-field at plane 1, obtained from the hologram at plane 2, in Figure 2a, compared to the measured benchmark in Figure 2b. The contour lines on each of these plots are separated by 5 dB increments. In both the reconstruction and benchmark level maps, the line enclosing the region of maximum level (above 135 dB) extends from approximately $z = 10$ to 18 m. A comparison of the contour lines also demonstrates that the level variation in the vertical direction is captured by the multi-source expansion, in spite of the fact that only the axisymmetric mode ($n = 0$) is used. Figure 2c shows the level difference between the benchmark and reconstructed levels over plane 1, and the black contour lines show the locations where ± 3 dB errors occur. Despite the limitation of this model to the $n = 0$ azimuthal mode, at 125 Hz the reconstruction error is less than 3 dB over almost all of plane 1, as shown by the outlined region of Figure 2c. Figure 2d-f is a similar reconstruction and benchmark comparison for 125 Hz, but at the arc location. The boundaries of the region that is within 5 dB of the maximum level, in the reconstruction, is between 130° and 150°+, and the benchmark shows a maximum-level region between 136° and 150°+. The error plot of Figure 2f shows that the error is less than 3 dB over most of the arc.
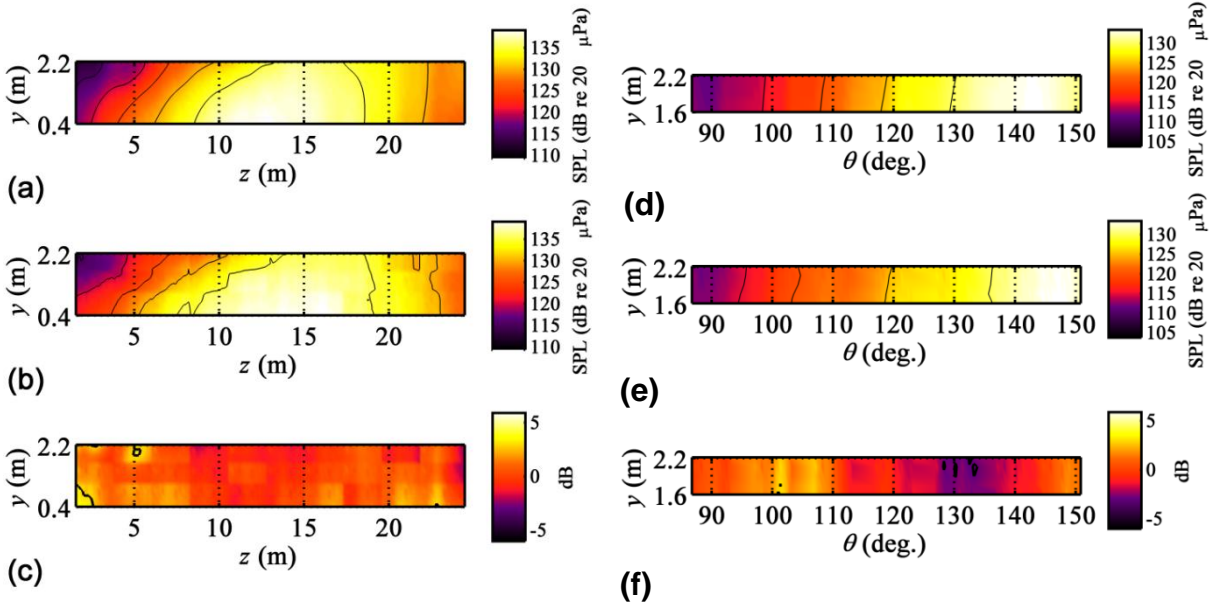
Figure 2: MSTR SONAH reconstructions at plane 1 and the arc for military power, 125 Hz. (a) Plane 1 reconstructed SPL. (b) Plane 1 benchmark measurement. (c) Difference between the reconstructed and benchmark levels in dB at plane 1. The black line outlines the region where the difference is less than 3 dB. Average error is 1.0 dB. (d) Arc reconstructed SPL. (b) Arc benchmark measurement. (c) Difference between the reconstructed and benchmark levels in dB at the arc. The black line outlines the region where the difference is less than 3 dB. Average error is 1.4 dB.

Figure 3 shows a reconstruction of the near-field region of the jet at 125 Hz, including over a half conical surface at the approximate location of the jet shear layer boundary and over a second surface with a uniform height of 1.9 m, which is the same height as the jet centerline. This demonstrates the overall directivity of the source, which, since the high-amplitude regions are accurately located at plane 1 and the arc, can be considered as a true representation. The fringe pattern in both the cone and planar surface is an artifact of the discrete spatial sampling and discrete wave-function representation.
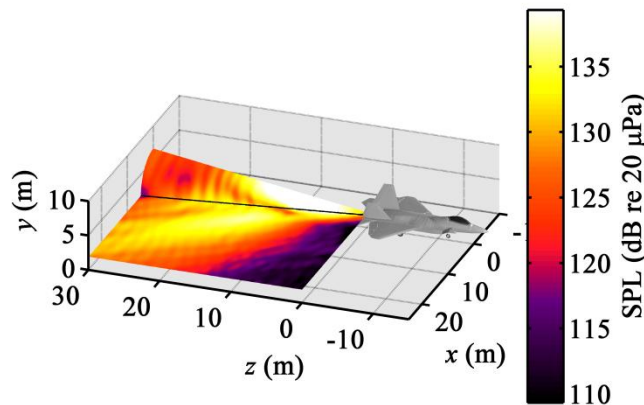
Figure 3: MSTR SONAH reconstruction in the vicinity of the jet for military power, 125 Hz. Levels are shown on a half conical surface (toward the side of the measurement) at the approximate location of the shear layer edge and over a plane at y = 1.9 m, the height of the centerline of the jet.

5. CONCLUSION

Sound field reconstructions of full-scale jets measured over concrete are possible through the MSTR SONAH method. Hence, it is not necessary to measure a full-scale jet in an anechoic environment or far from the ground, which would increase the cost and difficulty of a measurement. This paper has demonstrated the implementation of the MSTR SONAH method to the full-scale jet problem at a single frequency and engine condition. Further analyses of the jet noise properties at additional frequencies and engine powers will be described in the future.

It is well understood that jet noise is generated over a volumetric turbulent region. The type of errors introduced to the reconstructions of this study that are due to the assumption of a linear source at the jet centerline, as opposed to a volumetric source, is unclear. A future volumetric-source wave-field model would help to illuminate this issue. It is feasible that accurate source reconstructions can allow for the isolation of the reflection effects in the future,[20,21] which would allow for the generation of a free-field model of the source radiation. On a related note, it is difficult to quantify the accuracy of reconstruction in the region of the assumed hydrodynamic near field (i.e. on the conical reconstruction surface), without benchmark measurements, especially since the data were collected in the acoustic far field for many frequencies. Modified measurement techniques that allow for near-field measurements would result in improved verification, as well as more accurate near-field models.

ACKNOWLEDGMENTS

REFERENCES

[1]S. A. McInerny, G. Lu and S. Olcmen, "Rocket and jet mixing noise, background and prediction procedures", National Center for Physical Acoustics, University of Mississippi, 2004.

[2]V. Mestre, "Effects of aircraft noise: Research update on selected topics", Airport Cooperative Research Program, **Synthesis 9**, Project 11-03, Topic S02-01, 2008.

[3]J. Hald, "Basic theory and properties of statistically optimized near-field acoustical holography," *J. Acoust. Soc. Am.* **125**, 2105-2120 (2009).

[4]Y. T. Cho, J. S. Bolton and J. Hald, "Source visualization by using statistically optimized near-field acoustical holography in cylindrical coordinates," *J. Acoust. Soc. Am.* **118**, 2355 (2005).

[5]R. Steiner and J. Hald, "Near-field acoustical holography without the errors and limitations caused by the use of spatial DFT," *Int. J. Sound Vib.* **6**, 83-89 (2001).

[6]S. F. Wu, "On reconstruction of acoustic pressure fields using the Helmholtz equation least squares method," *J. Acoust. Soc. Am.* **107**, 2511-2522 (2000).

[7]T. Semenova and S. F. Wu, "On the choice of expansion functions in the Helmholtz equation least-squares method," *J. Acoust. Soc. Am.* **117**, 701 (2005).

[8]S. F. Wu, "Methods for reconstructing acoustic quantities based on acoustic pressure measurements," *J. Acoust. Soc. Am.* **124**, 2680-2697 (2008).

[9]S. F. Wu, "Techniques for implementing near-field acoustical holography," *Sound Vib.* **44**, 12-16 (2010).

[10]M. Lee and J. S. Bolton, "Source characterization of a subsonic jet by using near-field acoustical holography," *J. Acoust. Soc. Am.* **121**, 967-977 (2007).

[11]A. T. Wall, K. L. Gee, T. B. Neilsen, D. W. Krueger, M. M. James, S. D. Sommerfeldt and J. D. Blotter, "Full-scale jet noise characterization using scan-based acoustical holography," AIAA Paper 2012-2081, June 4-6, 2012.

[12]J. Hald, "Patch holography in cabin environments using a two-layer hand-held array and an extended SONAH algorithm," Proceedings of Euronoise 2006, 2006.

[13]A. T. Wall, K. L. Gee, M. M. James, K. A. Bradley, S. A. McInerny and T. B. Neilsen, "Near-field noise measurements of a high-performance military jet aircraft," *Noise Control Eng. J.* **60**, 421-434 (2012).

[14]D. Long, J. Peters and M. Anderson, "Evaluating turbofan exhaust noise and source characteristics from near field measurements," AIAA Paper 2009-3214, May 11-13, 2009.

[15]D. W. Krueger, *Array-based characterization of military jet aircraft noise* (M.S. Thesis, Brigham Young University, Provo, 2012).

[16]A. T. Wall, K. L. Gee and T. B. Neilsen, "Modified statistically optimized near-field acoustical holography for multi-source fields," *Proc. Mtgs. Acoust.*, (2013).

[17]A. T. Wall, *The characterization of military aircraft jet noise using near-field acoustical holography methods* (Dissertation, Brigham Young University, Provo, UT, 2013).

[18]A. T. Wall, K. L. Gee, M. D. Gardner, T. B. Neilsen and M. M. James, "Near-field acoustical holography applied to high-performance jet aircraft noise," *Proc. Mtgs. Acoust.* **9**, 040009 (2011).

[19]A. T. Wall, K. L. Gee, D. W. Krueger, T. B. Neilsen, S. D. Sommerfeldt and M. M. James, "Aperture extension for near-field acoustical holography of jet noise," *Proc. Mtgs. Acoust.* **14**, 065001 (2013).

[20]D. K. McLaughlin, C.-W. Kuo and D. Papamoschou, "Experiments on the effect of ground reflections on supersonic jet noise," AIAA Paper 2008-22, January 2008.

[21]C.-X. Bi and J. S. Bolton, "An equivalent source technique for recovering the free sound field in a noisy environment," *J. Acoust. Soc. Am.* **131**, 1260-1270 (2012).